Improved Paraffin-Deposition-Profile Estimation in Hydrocarbon Pipelines and Effective Mitigation Review

Sheikh Mohammad Samiur Rahman and **Sibi Chacko,** Heriot-Watt University

Summary

Flow of paraffinic hydrocarbon liquids within extended pipeline networks or wells, where the environment/bulk temperature is below the cloud point or wax-appearance temperature (WAT), could result in precipitation of wax from the bulk fluid. Precipitated wax crystals from crudes deposits on the inner pipe wall could lead to reduced flow area or even complete blockage and could present a costly problem in the production and transportation of petroleum products. Timely removal of such deposits is extremely important to avoid associated problems.

This paper illustrates a numerical approach to estimate the deposition profile and its effect on flow-related parameters. Later, the procedure is validated with field data from a North Sea offshore production facility. This paper also seeks to propose a feasible solution to avoid such flow-assurance issues; in doing so, current commonly practiced reduction and preventive methods are reviewed. Previously, providing thermal insulation with aerogel foam had proved to be the most effective option in preventing wax from precipitating. A relatively new approach is discussed in this paper, which allows for minimizing the usage of insulation material in an attempt to reduce the implementation cost of the proposed precaution. Theoretical implementation of the procedure was also conducted to identify its effectiveness, which was later found to be elimination of the deposition completely.

Introduction

Wax deposition in subsea pipelines or production facilities in cold environments poses a major threat to the economic development of petroleum industries. High WAT and pour point are the two factors having significant contribution to the deposition process. The heavier *n*-alkanes with higher carbon atoms tend to become insoluble as the temperature drops below the cloud point or WAT. The high-molecular-weight paraffin decreases as it deposits along the pipe surface during the flow, later forming wax crystals; however, the deposition of wax leads to the formation of gel. As a significant amount of oil gets trapped in the wax layer, it leads to gelling that inhibits flow by causing non-Newtonian behavior, which is highly unpredictable. The fraction of oil trapped is termed porosity and is usually assumed to be in the range of 60 to 90%. The deposition of paraffin could lead to well shut-in, pipeline replacement or abandonment, excess power consumption while pumping, equipment failures, and, of course, the enormous cost of prevention and remediation.

Background

To overcome wax-deposition-related flow-assurance challenges, accurate estimations of the deposition processes are highly recommended. Researchers have already made significant progress in understanding the thermodynamic equilibrium and deposition mechanisms of wax. Aiyejina et al. (2011) reviewed the current state of research, highlighting what is understood to date about the mechanisms guiding wax deposition and how the knowledge could be applied to modeling and providing solutions to such problems, together with providing a brief understanding of the deposition process and the mechanisms responsible for the deposition process. Rygg et al. (1998) illustrated the major development on the Rygg-Rydahl-Rønningsen (RRR) model for estimating wax deposition in wells and pipelines, while incorporating the variation of hydraulic diameter caused by wax deposition. The model has been validated by applying it to a number of single-phase, multiphase wells and pipeline networks. Rosvold (2008) conducted a single-phase laboratory-scale flow-loop experiment on a typical waxy gas condensate, and later, an identical simulation case was created with a commercial steady-state preprocessor flow simulator. The simulations were conducted with three different wax-deposition models and were later verified with laboratory results. Lindeloff and Krejbjerg (2002) presented a new algorithm for calculating deposition of wax in a pipeline system and demonstrated it on a multiphase case, which was already considered by Rygg et al. (1998). The simulated results predicted higher deposition, and the pressure drop did not agree with field data explained by Rygg et al. (1998). Despite the unmatched results, they conducted a compositional analysis on the pseudocomponents (wax/paraffin) that seems to agree with the general trend of the wax-deposition profile. Labes-Carrier et al. (2002) provided a brief guideline on the procedure for conducting a wax-deposition simulation using the RRR model. The analysis was performed on the basis of a gas condensate and a stabilized oil sample from the North Sea. The literature explains the steps such as fluid-composition characterization, tuning parameters for fluid, and generating necessary data required before conducting the simulation. Denniel and Blair (2004) provide a detailed understanding on the evolution of the aerogel-material manufacturing procedure over the past few decades. Together with its insulation properties, Denniel and Blair also elaborate about the reliability of aerogel as an ideal insulation material for pipes. The most suitable method for insulating a pipe section using an aerogel blanket was proposed as the pipe-in-pipe (PIP) technique in which a blanket of aerogel solid is placed between two layers of pipe. Experiments were conducted on its thermal conductivity during compression and aging at extreme temperatures.

The RRR Model. The deposition model is fundamentally a steady-state compositional pipeline simulator, in which a steady-state approach is chosen because wax deposition is a very slow process relative to typical residence time (local flow disturbances). To perform the simulation, it is necessary to split the pipeline into a number of sections in which the pressure and compositions are assumed to be constant. The deposition model calculates the wax deposition along the pipe wall and the viscosity of the composition continuously, from which pressure drop and temperature are calculated by

Original SPE manuscript received for review 21 August 2012. Revised manuscript received for review 30 April 2013. Paper (SPE 165933) peer approved 10 May 2013.

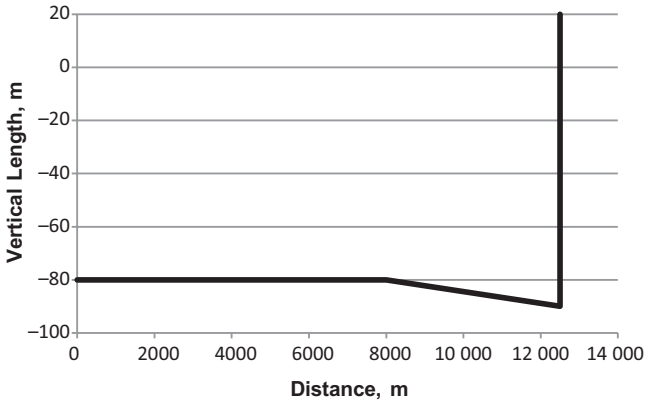

Fig. 1—Pipeline and riser profile.

integration in time. The model is currently based on four different submodels as listed below:

- Flow model: used for estimating steady-state pressure drop, liquid holdup, and flow-regime transitions
- Thermodynamic wax model: determines the number and properties of the different phases for each section of the pipe
- Viscosity model: calculates the viscosity
- Wax-deposition model: predicts the amount of wax deposition

Besides the submodels, the mechanisms considered to have a significant impact on the deposition of precipitated wax, were expressed in mathematical relationships. Major mechanisms governing the deposition of wax are identified as

- Shear-dispersion mechanism: This contributes to wax deposition through the lateral motion of particles immersed in a shear flow, thus the precipitated wax is transported from the turbulent core to the pipe wall.
- Molecular-diffusion mechanism: As a result of the surrounding cold environment, the hydrocarbon stream flowing in a pipeline is cooled; the pipe wall reaches the wax-appearance point (WAP), initiating the molecular-diffusion process. At that temperature, the oil is saturated with wax in solution and wax starts precipitating out. Wax precipitation leads to a concentration gradient between dissolved wax in the turbulent core and the wax remaining in the solution at the wall. Because of this, dissolved wax diffuses toward the wall, where it is subsequently deposited.

Total wax deposition is estimated considering both the shear-dispersion and molecular-diffusion mechanisms, leading to the total rate of increase in thickness of the wax layer. However, there were assumptions made for this model such as the precipitation rate at the wall not being a limiting factor, and that all wax transported to the pipe wall would stick to the surface as long as the temperature was less than the WAT. This clearly indicates that there are no removal mechanisms implemented in this model. The model has been applied on two different cases, which were discussed by Rygg et al. (1998), and good agreements were observed with the field data.

OLGA® 7

The analysis will be highly focused on the usage of OLGA 7 (SPT Group 2013), a steady-state and transient simulation program for multiphase petroleum production systems. The integrated three-phase module focuses on gas, oil, and water, and separate conservation equations are applied at each phase of the mixture. During the present analysis, the subjected fluid will not contain any aqueous component and thus only two-phase flow will be simulated. The module also allows transition between two different flow regimes: distributed and separated flows. The wax module, on the other hand, allows modeling of wax precipitation and deposition of wax by use of the RRR model developed by Rygg et al. (1998). The model takes into account the thermal-hydraulic effects of the wax in the following way:

- Mass-conservation equations are solved for wax dissolved, precipitated, dispersed in oil, and deposited on the wall.
- Pipe diameter, roughness, and wall heat transfer for each pipe section are adjusted as wax deposits on the wall.
- Heat balance and volume change because of precipitation, deposition, and melting of wax.

TABLE 1—PIPELINE MATERIAL SPECIFICATIONS AND BOUNDARY CONDITIONS FOR CASE A

Pipe construction material	14-mm thickness of steel 1-mm thickness of paint 6-mm thickness of concrete
Pipe internal diameter	0.1905 m
Inlet pressure	30 bar
Inlet temperature	70°C
Flow rate	15.55 kg/s

PVTsim® (Calsep 2008). On the basis of the plus fraction of the fluid, it is possible to conduct a compositional analysis to generate extended compositional data to perform accurate pressure/volume/temperature (PVT) and phase equilibrium calculations. The thermodynamic software tool PVTsim is able to perform such a characterization procedure based on the molecular weight and density of the plus fractions. PVTsim is a necessary first step for using OLGA 7 and has significant influence on simulation results. Using PVTsim, data files containing the PVT properties of the fluid and the properties for the wax-forming components will be generated.

Case A

The multiphase case discussed by Rygg et al. (1998) will be recreated during this analysis. The case consists of a water-free multiphase oil/gas well stream being transported from a subsea template to a North Sea platform. To recreate the scenario, pipeline layout, material properties, ambient conditions, and flow conditions were kept identical. The pipeline comprises a 12.5-km near-horizontal section followed by a 110-m riser section, as plotted on **Fig. 1.** However, the horizontal section of the pipeline was trenched and the depth of trenching was approximated through a parametric study on the basis of the available field data. The ambient temperature of the seabed was considered to be constant at 5°C, and the kinetic energy of the ambient fluid flow was assumed to be negligible because the flow had very minor velocity. Detailed system data and conditions have been tabulated in **Table 1.**

Apart from the boundary conditions and pipe-profile data, it is equally important to characterize the fluid using PVTsim, because a laboratory experiment could not be conducted for characterizing the fluid. The composition data of the plus fraction fluid was obtained from the Case-A scenario respective to the current North Sea production system (as tabulated in **Table 2**). The thermodynamic tool PVTsim used for characterizing the fluid uses an approach similar to that described by Pedersen et al. (1992). Based on the C_{10+} fraction of the fluid, the extended composition was estimated to C_{80} by PVTsim. Various thermodynamic models are available for estimating WAT or the wax-precipitation curve (i.e., wt% of solid wax as a function of temperature at different pressures). Such models are also integrated into PVTsim and have been applied in the current analysis.

Tuning in PVTsim. It is very likely that the software predicts the WAP accurately, and, therefore, a need for tuning the WAP with experimental results has always existed. **Fig. 2** shows the differ-

TABLE 2—CASE A FLUID-COMPOSITION DATA			
Component	Mol %	MW* (g/mol)	Density (g/cm^3)
N_2	1.030	28.014	
CO_2	1.200	44.010	
CH_4	16.180	16.043	
C_2H_6	4.550	30.070	
C_3H_8	8.260	44.097	
i-C_4H_{10}	1.520	58.124	
n-C_4H_{10}	5.370	58.124	
i-C_5H_{12}	2.290	72.151	
n-C_5H_{12}	3.020	72.151	
C_6	3.980	85.100	0.6640
C_7	6.000	93.200	0.7320
C_8	5.790	107.100	0.7500
C_9	3.860	119.700	0.7700
C_{10+}	36.950	286.000	0.8840

*MW = Molecular Weight

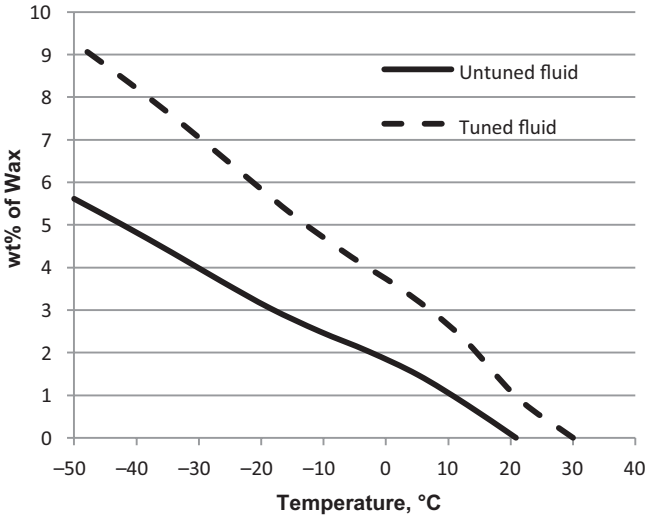

Fig. 2—WAT profile obtained before and after tuning within PVTsim.

TABLE 3—EXPERIMENTAL VS. PVTsim-GENERATED WAT AND OIL-VISCOSITY DATA POINTS		
WAP	Software estimated at 30 bar	20.84°C
	Tuned at 30 bar	30.00°C
Viscosity of the oil	Software estimated at 1 bar	3.31 cp at 70°C
		13.68 cp at 0°C
	Tuned at 1 bar	2.33 cp at 70°C
		11.61 cp at 0°C

ences of the WAP and profile of the WAT curve predicted by the software vs. the tuned WAP with experimental data. Tuning the WAT parameter alters the profile of the curve, making it steeper. Untuned WAP affects the results obtained for the wax-deposition profile in the pipeline greatly, causing it to underestimate the deposition thickness. Similarly, the viscosity data for the oil needs to be tuned with the laboratory results, thus enabling the software to predict accurately the non-Newtonian behavior or the shear rate of the fluid once the wax begins precipitating out from the bulk fluid. Inaccurate viscosity data would lead to unreliable pressure drop in the pipeline during simulation. The viscosity tuning of the current composition was limited to a function of temperature and pressure resulting from lack of experimental data. A basic presentation of the tuned and untuned parameters is noted in **Table 3.**

Discretization of the Flowline. Once the case was fully set up, a test run was performed to identify those sections with maximum variation of deposition thickness. On the basis of these results, the length of the pipeline was divided efficiently into 40 sections (i.e., the number of sections was greater where maximum variation of wax thickness was observed and vice versa). On the other hand, to avoid instabilities in the simulated results, the neighboring-section length ratios were kept between 0.5 and 2.

Results and Discussion. The initial simulation was expected to generate results in agreement with Rygg et al. (1998). while maintaining the default parameter values of the diffusion coefficient (D) multiplier and porosity, which were 1 and 60% respectively. Even though the deposition curve and the pressure-drop profile demonstrated a profile similar to that observed by Rygg et al., it was found to be underestimating by a scale of 25%. Therefore, a second simulation was conducted with an increased diffusion coefficient (D) multiplier of 1.5 and with the remaining parameters the same as those reported by Rygg et al. The deposition-thickness profile is plotted in **Fig. 3.** A higher deposition thickness is observed, and the peak sections of the deposition are a close match to the results obtained by Rygg et al. (1998). These results agree with the literature discussed in the previous sections of this report. Wax starts depositing at approximately 6.175 km from the upstream of the flowline (also observed by Rygg et al.), and if the starting point of the deposition is correlated with the temperature profile of the bulk fluid and inner-pipe-wall temperature **(Fig. 4)**, it is found that the inner-pipe-wall temperature attains the WAT at the initiation point of wax deposition. An important point to note during the analysis is that wax does not deposit until WAP is attained by the inner pipe

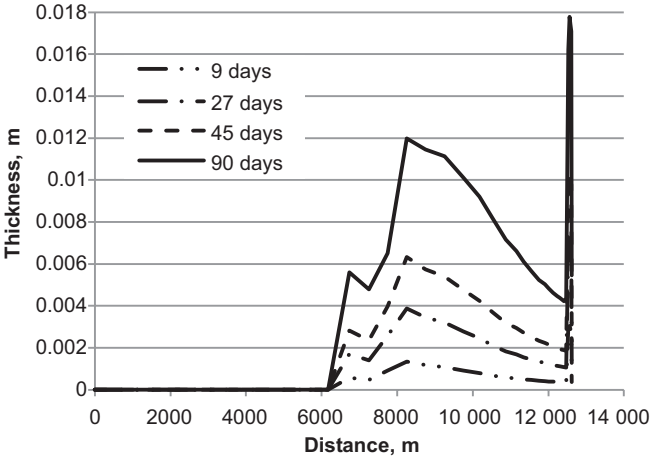

Fig. 3—Deposition-thickness profile plotted with a diffusion-coefficient multiplier of 1.5.

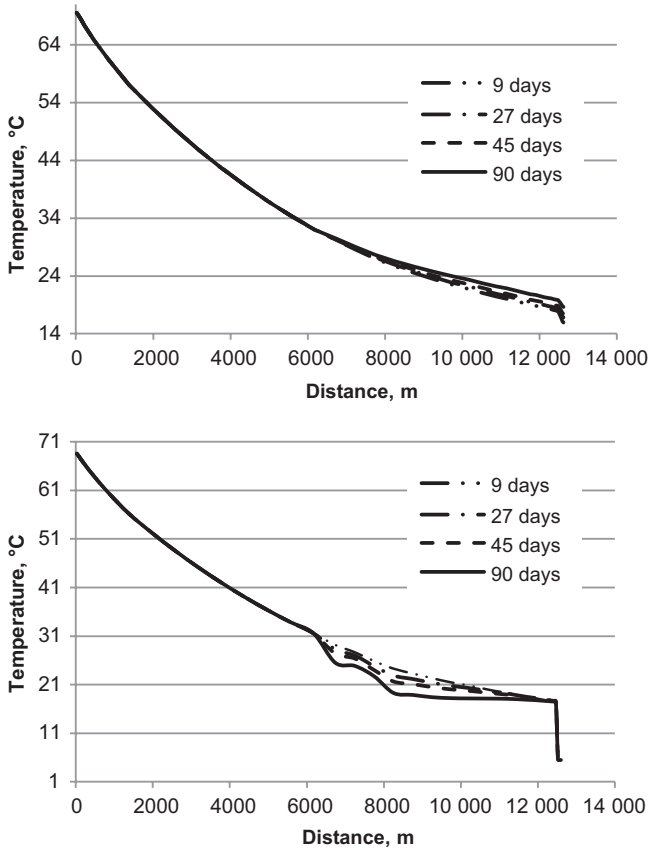

Fig. 4—Inner-pipe-wall temperature profile (bottom) vs. bulk-fluid temperature profile (top).

wall; a similar claim was also made by Rosvold (2008). A compositional analysis was conducted by Lindeloff and Krejbjerg (2002) to explain the profile obtained in the horizontal section of the pipe. It was identified that the heavier pseudocomponents tend to deposit faster as the WAP is achieved, whereas the lighter components tend to travel farther and deposit thereafter. However, another observation that needs to be focused on is the effect of heat loss from the bulk fluid, which tends to reduce as the deposition builds, as demonstrated by the temperature curves. The bulk fluid temperature at the downstream of the pipeline tends to attain a higher temperature over time; on the other hand, inner-pipe-wall temperature drops over time. The formation of wax at the pipe wall acts as an insulation layer, thus minimizing the heat loss from the bulk fluid. It also explains the shifting of the peak deposition at the horizontal section of the pipe toward the downstream over time. The maximum deposition is predicted at the riser section, as a result of the rate of heat transfer, which is comparatively higher at the riser section because of lack of trenching and limited insulation. This results in a much steeper temperature-profile drop and causes thicker deposition.

The pressure profile is plotted in **Fig. 5,** illustrating the effect of wax deposition on pressure drop. The near-vertical section of the profile indicates the pressure drop caused by hydrostatic head at the riser section, although the effect of deposition has considerable impact on the pressure drop at the downstream. The obvious reason for such a pressure drop over time is the reduction in hydraulic diameter or effective pipe diameter because of deposition buildup. The pressure drop at the outlet over the 90-day period was observed to be 1.5 bar, which is quite moderate and also in reasonable agreement with the field data discussed by Rygg et al. (1998). On the other hand, similar observations were made in Rygg et al. (1998) on the wax-deposition profile, in which the deposition begins at approximately 6.25 km from the upstream and obtains a peak at the riser section.

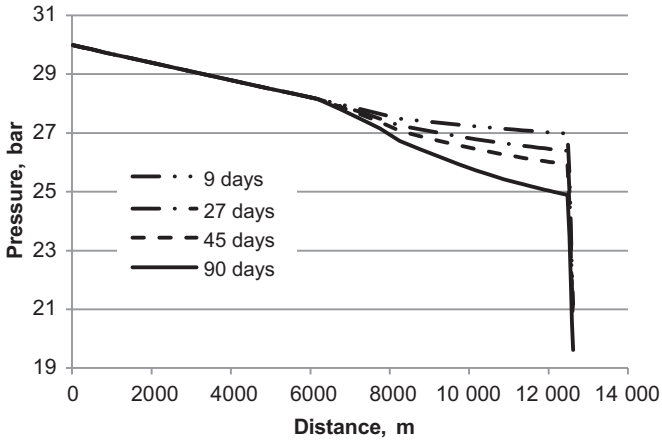

Fig. 5—Pressure-drop profile plotted with diffusion-coefficient multiplier of 1.5.

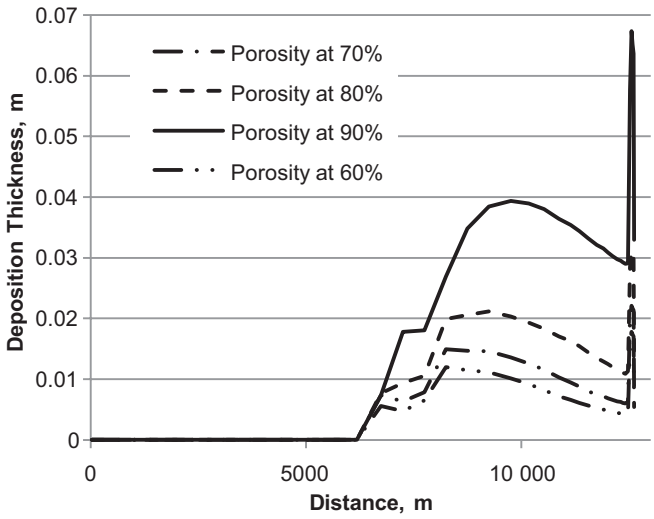

Fig. 6—Variation of the deposition profile with varying porosity.

Sensitivity Analysis. ***Porosity.*** Because the porosity of the deposited wax is defined as the space between the wax crystals occupied by trapped oil, a high porosity value should mean a higher amount of oil is being captured between the wax crystals. As a result of the increase of trapped oil, it is estimated to have higher deposition thickness, which was proved through a simulation at a later stage **(Fig. 6).** For Case A, the simulation was performed for 90 operational days and with a porosity of 60% because similar assumptions were made by Rygg et al. (1998). As the porosity was increased, the deposition thickness also increased (i.e., the rate of precipitation of solid wax increased with increasing porosity), although the linear relationship was not. However, it was claimed by Labes-Carrier et al. (2002) that higher porosity should result in a softer deposit and vice versa, which was proved when the observation of this analysis shifted toward the parameter called "specific wax mass at wall." Such an analysis could provide information for optimizing pigging frequency and designing a suitable pig block.

Effect of Insulation on Deposition. From the preceding analysis, it was acknowledged that the initiation point of the deposition correlates directly with the instance in the inner-pipe-wall temperature profile at which the WAT was achieved. This gives the aim for the current sensitivity analysis to observe the effect of delaying the WAT on the wax-deposition profile. An effective way of delaying the WAT is by insulating the pipeline with a material of lower thermal conductivity. Therefore, a parametric study was set up while slightly modifying the current scenario. At the hor-

TABLE 4—STANDARD THERMAL SPECIFICATIONS FOR MATERIALS AT OPERATING CONDITIONS FOR CASE A

Material	Specific Heat Capacity (J/kg-°C)	Thermal Conductivity (W/m-°C)	Density (kg/m^3)
Aerogel foam	1150	0.012	100
Polyurethane foam	1500	0.025	30
Microporous material	800	0.019	230
Polypropylene foam	2000	0.17	750
Dry air	1.005	0.0257	1.205
Concrete	880	1.8	2250
Seabed sand	1250	2	1750
Paint	2300	3.2	1500
Steel	500	50	7850

izontal section of the pipeline, the trenching depth was replaced with a polypropylene foam, the thickness of which varied from 30 to 120 mm. Thermal properties of the polypropylene foam are presented in **Table 4.** However, it should be noted that the aim of this study is purely to understand the effect of WAT on deposition, and thus the scenario created for this analysis is completely irrelevant to the real scenario. A detailed analysis on this is covered in the later sections of this paper.

The scenario was simulated for 20 operational days, and the results have been plotted on **Figs. 7 and 8;** a clear understanding was acquired on the effect on the deposition profile by varying WAT. A statement can now be made that the major driving force for the wax deposition is the temperature profile. Thicker insulation delays the WAT farther down the flowline and, in turn, results in pushing the deposition-initiation point farther downstream. Higher deposition peak was observed at the riser section because the wax content in the bulk fluid remained high as a result of the deposition being delayed. A larger temperature gradient was observed at the riser despite equal insulation of the entire pipeline.

The comparison was conducted with an insulation material of constant thickness at both the horizontal and the riser section because trenching of the pipeline was not incorporated during the current analysis. In certain scenarios, the temperature drop in the riser and horizontal section of the pipeline was expected to have a continuous exponential drop in temperature profile, whereas the profile obtained after simulations demonstrated an exponential temperature drop in the horizontal section of the pipe and a steeper temperature drop at the riser section. With further literature review, it was identified that the Joule-Thomson effect was influencing the temperature profile in the riser section. The Joule-Thomson effect is a thermodynamic process that occurs when gas expands from high pressure to low pressure at constant enthalpy and, in the process, reduces the temperature of the fluid. Similar observations were reported at multiple riser sections by Gloaguen et al. (2007). Thus, the effect of Joule-Thomson cooling cannot be prevented by insulation.

Prevention of Deposition

Thermal Insulation. With more-recent exploration of oil and gas, production facilities are shifting toward adverse operating conditions, hence traditional insulation systems are proving to be less effective. Using conventional material for meeting current insulation demands in subsea pipelines could mean an excessively thick coating of insulation material, which may cause manufacturing concerns as well as reducing vessel capacity. Attaining a lower overall heat-transfer coefficient (OHTC) is a challenging task, especially for a deep-sea pipeline. Some of the most common materials used to overcome such a challenge are

1. Aerogel
2. Polyurethane
3. Microporous material
4. Polypropylene

Aerogel Material. Aerogel is a synthetic porous material derived from a gel in which the liquid component of the gel is replaced with gas. The material has been in existence since 1931 and has proved to have attractive physical properties such as high temperature resistance, very low thermal conductivity, light weight, sound proof and high-impact energy absorption. Despite the desirable properties of the material, mass production of aerogel was not possible for industrial usage until the recent development of a revolutionary aerogel manufacturing procedure. The production time for a single

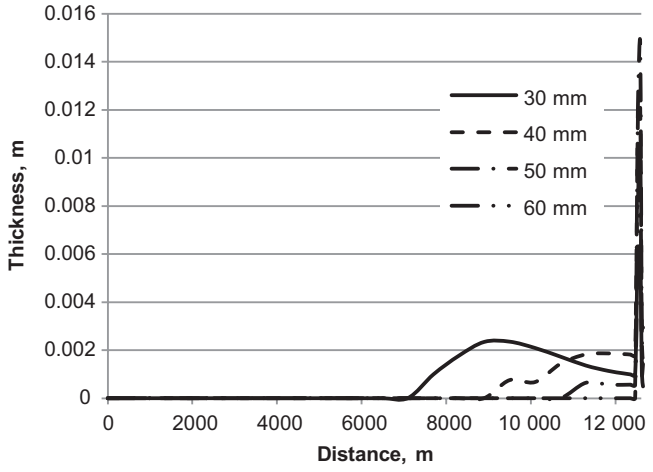

Fig. 7—Effect of insulation on deposition profile.

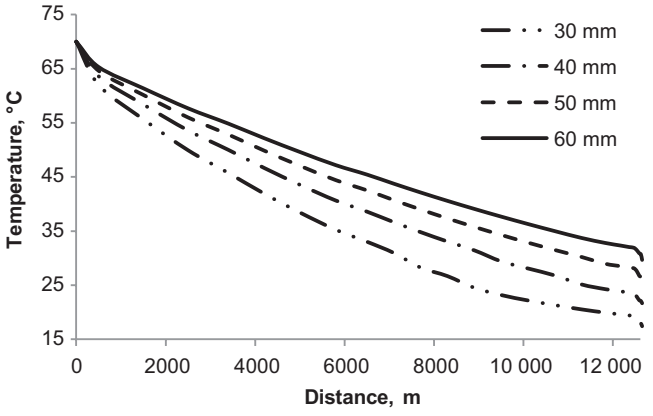

Fig. 8—Effect of insulation on inner pipe wall.

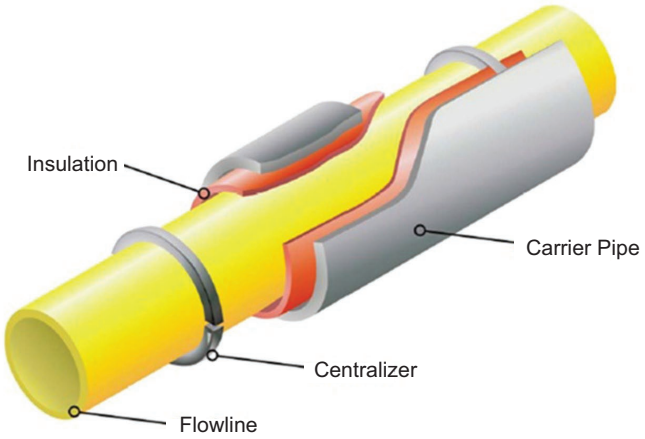

Fig. 9—PIP arrangement with insulation layer.

batch of aerogel material during the 1930s was 4 months, and by 2002, it was reduced to just under 4 hours (Denniel and Blair 2004). Because of the new manufacturing technique, the material is being produced at affordable prices for industrial usage. Thus, the focus of this analysis will be mainly on aerogel insulation and illustrating the reasons for aerogel being the best choice for subsea insulation.

However, it is essential to carry out laboratory-scale tests to observe its performance on worst-case scenarios. Similar tests were discussed by Denniel and Blair (2004) in which the material was tested for the effect of aging and compression on thermal conductivity. The thermal conductivity of the aerogel material was measured after exposure to strain levels in the range of 10 to 20% and relaxation; very negligible change in thermal conductivity was recorded. Similarly, for the aging test, three different samples of the material were placed inside an oven for 8 weeks and maintained at a temperature of 180°C. Surprisingly, further reduction of thermal conductivity was recorded over time, which makes it more suitable for long-term usage.

Insulation for Reelable PIP Configuration. Although the insulation materials have very low thermal conductivity, exposing them directly to the subsea environment will greatly affect their insulation properties and cause permanent damage to the material. Therefore, a configuration such as a PIP section (in which a pipe is inserted into another pipe and the created intermediate annulus can be used to place an insulation material) is highly recommended for installing insulation materials for deepsea applications. Thus, the insulation material is protected by the carrier pipe from hydrostatic pressure and from water absorption. Typical arrangement of a PIP section is displayed in **Fig. 9.** For protection of the integrity of the insulation material, centralizers are used.

Because it is too early to fix apropriate dimensions for the carrier pipe and insulation thickness, a detailed study on efficient use of insulation and its optimum thickness needs to be identified. However, the flowline material, its outer diameter (OD), and its thickness need to be kept unaltered. Changing those parameters will require an updated boundary condition for the effluent, and panumatic pressure testing will need to be conducted because pressurized fluids are being flown.

Efficient Insulation. As mentioned by Rygg et al. (1998), changing the operating pressure of the fluid has an impact on its WAP. Additionally, the scenario specified in Case A had a variation in fluid pressure (Fig. 5) within a range of 30 to 21.3 bar throughout the pipeline before wax crystals began settling at the wall. The WAT was simulated for the operating pressure range using PVTsim. However, the change in WAT was observed to be very minor (less than 0.5°C) within the pressure range; thus, its effect can be assumed to be negligible during this analysis.

A basic comparison is conducted between aerogel and other widely used insulation materials for offshore pipeline insulation by use of the PIP teqnique through a few sets of parametric studies. The objective is to obtain the optimum thickness for each insulation material, which is required if the entire flowline is to be insulated to keep the inner-wall outlet temperature of the pipe section 20% higher than the WAT, which is approximately 38°C for Case A. The 20% is considered as an optimum safety factor because the simulations were conducted in a steady-state manner and the ambient conditions at deep sea are assumed to be constant; although, in reality, the conditions ought to vary. Thus, to compensate the variation, outlet temperature of the inner pipe wall is recommended to be kept 20% higher than the WAT. This safety factor will be considered throughout the analysis.

The results obtained at the end of the parametric study are displayed in **Table 5.** It is clear that using conventional polypropylene foam would require the thickest insulation and would have a great impact on the bulkiness of the pipe section. Thicker insulation would require a carrier pipe with a larger OD, increasing its material cost in addition to its logistics and installation costs. However, aerogel reduces the insulation requirements dramatically, thus minimizing all associated problems. The comparison clearly shows the reason for aerogel being the best choice for an insulation material.

Optimizing Material Layout. It has been proved that applying an insulation of aerogel material with a thickness of 4.7 mm can successfully maintain the inner-pipe-wall temperature at 20% over the WAT of the fluid, and on the basis of the heat loss from the fluid, the global OHTC is approximated to be 2.9 W/m^2·K by use of Eq. 1. However, with an aerogel insulation thickness of 4.7 mm, the calculated volume of aerogel material required for covering the entire pipeline is 41.64 m^3. Although its price is dropping as manufacturing processes are becoming more feasable, aerogel still remains relatively more expensive than other conventional insulation material. This subsection will demonstrate a procedure to efficiently insulate the pipeline as well as reduce insulation-material usage. Because the focus of this paper does not extend to strength analysis of the pipeline, a suitable steel carrier pipe with dimensions based on American Petroleum Institute (API) standards has been selected to avoid further buckling and reeling analysis.

$$OHTC = \frac{Q}{ID \times \pi \times (T_b - T_{out})}, \quad \text{.....(1)}$$

Where ID is pipe inside diameter.

TABLE 5—LISTS THE MINIMUM INSULATION THICKNESS REQUIRED TO KEEP THE OUTLET TEMPERATURE 20% ABOVE WAT

Material	Thickness (mm)	Inner-Wall Temperature at Exit (°C)
Polypropylene foam	92	38.4
Polyurethane foam	10	37.9
Microporous material	8	39.4
Aerogel foam	4.7	37.9

TABLE 6—API STANDARD STEEL CARRIER-PIPE DIMENSIONS OBTAINED FROM MANUFACTURER

Type	OD (mm)	Wall Thickness (mm)	Available Insulation Thickness (mm)	Weight Per Meter (kg/m)
1	244.48	7.92	5.23	32.30
2	273.05	18.64	8.635	79.20
3	273.05	20.24	7.035	85.30

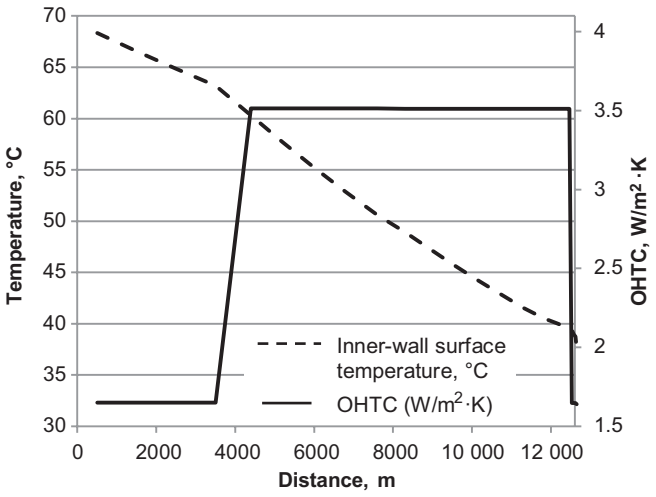

Fig. 10—Inner-pipe-wall temperature profile and local OHTC plotted for optimized run.

As has been illustrated (from **Table 6**), the minimum thickness of aerogel insulation required is 4.7 mm, which makes Type 2 a good choice of carrier-pipe dimension. The aim is to use the available insulation thickness for Type 2 carrier pipe while keeping the global OHTC of 2.9 W/m^2·K as an optimum target, because obtaining a higher global OHTC will result in a lower inner-wall temperature at the outlet and a lower OHTC will increase the usage of insulation material. Therefore, designing an efficient aerogel insulation system and reducing the insulation material required were based highly on the global OHTC variable.

Dry air could prove to be a very cheap alternative to aerogel but would not eleminate the need for aerogel. The idea is to use dry air as a secondary insulation material together with aerogel. The difference between dry air and conventional air is the percentage of moisture content. Dry air is usually known for having a lower moisture content and thus having a comparatively lower dewpoint than conventional air. Lower dewpoint is essential because the pipe walls in contact with dry air are expected to attain lower temperature, which could influence condensation from the air, thus affecting the insulation performance. Air-tight centralizers are recommended to prevent dry air from escaping once it is injected into the insulation gap during an on-vessel welding operation. Accurate calculation is required to identify the optimum length of the pipeline that needs to be insulated with aerogel. The rest of the pipeline would be insulated by use of dry air. The arrangement should be such that the global OHTC is averaged at 2.9 W/m^2·K. Thus, a test simulation was set up with the first 8 km of the pipeline and riser insulated with aerogel while the remaining length was insulated with dry air at 1 atm. The results indicate that the average local OHTC for the aerogel- insulated region (L1) is 1.64 W/m^2·K and for the air-insulated region (L2) is 3.51 W/m^2·K. Eq. 2 was formulated to calculate the global OHTC, which was later found to be 2.31 W/m^2·K. This value is lower than the target OHTC of 2.9 W/m^2·K, indicating that there is yet room for cutting down the insulation material required by reducing the aerogel-insulated length.

$$OHTC = \frac{(L1 \times A) + [L2 \times (100 - A)]}{100} \quad \text{.....(2)}$$

Eq. 2 was used to calculate the percentage of length required to be insulated by aerogel while keeping the OHTC at 2.9 W/m^2·K; the percentage was found to be 32.5%. This results in 4.098 km of the pipeline that needs to be insulated by aerogel and the remaining part by dry air. The calculated length was divided at the upstream section and the riser section of the pipeline; the scenario was resimulated with the updated specifications of the pipeline. The results have been plotted in **Fig. 10.**

According to Fig. 10 and **Table 7,** the inner-pipe-wall temperature-profile plot illustrates that outlet temperature was successfully kept at 38.8°C, an acceptable range, while the global OHTC remains at 2.9 W/m^2·K, as targeted previously. The volume calculated for the aerogel material required to cover 32.5% of the pipeline with 8.635-mm thickness was reduced to 25.32 m^3, which is 39.2% less aerogel-insulation volume than if the entire pipeline had to be insulated with 4.7-mm thickness.

Conclusions

A numerical approach was discussed throughout this analysis, providing a complete solution to a certain flow-assurance-related problem that exists within the petroleum industry. The following conclusions were made on the basis of the results:

- The commercially available flow- and heat-transfer-analysis software demonstrated its capability of carrying out steady-state simulation on the basis of the RRR model. The software was used to recreate the scenario of an existing offshore production facility. Several tuning parameters were uncovered and observed to have great effect on the profile and the nature of

TABLE 7—SUMMARIZED SIMULATION RESULTS OBTAINED FOR TEST AND OPTIMIZED RUN

Simulation	Local 1 (Aerogel Section; Cabot Aerogel 2012)		Local 2 (Dry-Air section)		Global OHTC (W/m^{2}K)	Outlet Temperature (°C)	Aerogel Volume Used
Test run	OHTC	1.65	OHTC	3.5	2.31	43.25	49.97 m^3
	Length (m)	8110	Length (m)	4500			
Optimized run	OHTC	1.65	OHTC	3.51	2.9	38.8	25.32 m^3
	Length (m)	4110	Length (m)	8500			

deposition. During the current analysis, parameters were tuned on the basis of available field data and previous simulated results; however, for alternative cases, such data might not be present, thus a laboratory-scale flow-loop setup was recommended to identify such tuning parameters. It was concluded that one of the major driving forces for wax precipitation was associated with the inner-pipe-wall temperature and keeping the wall temperature greater than the WAT, which successfully delays the deposition. This acts as a precursor for the development of the solution for the later sections of the paper. The current analysis was conducted on the basis of standard values and several approximated parameters. Secondly, the validation was based purely on pressure-drop field data, which can be very unreliable. Therefore, laboratory experimental setups, in which all conditions would be known and take-out sections could be attached along with the test flow loop to obtain accurate deposition-profile measurement, are highly recommended.

- A brief review was conducted of current-practice methods for reducing or preventing wax deposition; thermal insulation proved to be the best choice. Multiple insulation materials were proposed; aerogel material seemed to be the most-preferable option. However, a concrete solution was needed to preserve the material under water, and thus use of a PIP section was recommended. The use of dry air within PIP insulation, which is a relatively new idea, was suggested in this section. The idea, however, does not eliminate the use of aerogel but reduces the insulation-material usage by approximately 40% for the current case. Although the implementation of such an idea would be very limited, if the inlet temperature of the fluid is close to the WAT, then direct electric heating of the flowlines would need to be implemented. The approach of balancing global OHTC proved to be a very effective method for calculating the amount of insulation required. Eq. 2 was derived to calculate the percentage of length required to insulate a single pipeline with two different insulation materials to attain the targeted global OHTC.
- Although the current analysis fulfills the objectives it aimed for, it is still a time-consuming approach. Therefore, a continuous or discrete optimization technique could be implemented that would be universally applicable to any pipeline network regardless of the number of branches.

Nomenclature

A = percentage of length required to be insulated by aerogel material
D = diffusion coefficient
MW = the molar weight of wax component i, kg/mol
Q = radial heat-transfer rate
T_b = bulk-fluid temperature
T_{out} = outer-wall temperature of the pipe section

Acknowledgments

We would like to thank SPT Group for providing OLGA® 7 software and Jawad Azeem from Calsep for providing the PVTsim® Wax module, which were essential tools for completing this analysis successfully. We are also very grateful to Magnus Hebnes, General Manager and Senior Vice President of SPT Group, for accepting our request and offering us all the support required.

References

Aiyejina, A., Chakrabarti, D.P., Pilgrim, A. et al. 2011. Wax formation in oil pipelines: A critical review. *Int. J. Multiphase Flow* **37** (7): 671–694. http://dx.doi.org/http://dx.doi.org/10.1016/j.ijmultiphaseflow.2011.02.007.

Cabot Aerogel. 2012. Oil & Gas Insulation: Best-in-class insulation performance for pipe-in-pipe systems, http://www.cabot-corp.com/Aerogel/Oil-and-Gas-Insulation (accessed 02 March 2012).

Calsep. 2008. PVTsim (PVT simulation program), http://www.pvtsim.com.

Denniel, S. and Blair, C. 2004. Aerogel Insulation For Deepwater Reelable Pipe-in-Pipe. Presented at the Offshore Technology Conference, Houston, 3–6 May. OTC-16505-MS. http://dx.doi.org/10.4043/16505-MS.

Gloaguen, M., Bourdillon, H., Roche, F. et al. 2007. Dalia Flowlines, Risers, and Umbilicals. Presented at the Offshore Technology Conference, Houston, 30 April–3 May. OTC-18543-MS. http://dx.doi.org/10.4043/18543-MS.

Labes-Carrier, C., Rønningsen, H.P., Kolnes, J. et al. 2002. Wax Deposition in North Sea Gas Condensate and Oil Systems: Comparison Between Operational Experience and Model Prediction. Presented at the SPE Annual Technical Conference and Exhibition, San Antonio, Texas, USA, 29 September–2 October. SPE-77573-MS. http://dx.doi.org/10.2118/77573-MS.

Lindeloff, N. and Krejbjerg, K. 2002. A Compositional Model Simulating Wax Deposition in Pipeline Systems. *Energy Fuels* **16** (4): 887–891. http://dx.doi.org/10.1021/ef010025z.

OLGA v. 7.2.3. 2013. Kjeller, Norway: Scandpower Petroleum Technology (SPT Group). http://www.sptgroup.com/en/Software-Downloads/OLGA/

Pedersen, K.S., Blilie, A.L., and Meisingset, K.K. 1992. PVT calculations on petroleum reservoir fluids using measured and estimated compositional data for the plus fraction. *Ind. Eng. Chem. Res.* **31** (5): 1378–1384. http://dx.doi.org/10.1021/ie00005a019.

Rosvold, K. 2008. *Wax Deposition Models*. MS thesis, Department of Petroleum Engineering and Applied Geophysics, Norwegian University of Science and Technology (NTNU), Stavanger, Norway (June 2008).

Rygg, O.B., Rydahl, A.K., and Rønningsen, H.P. 1998. Wax deposition in offshore pipeline systems. *Proc.,* 1st North American Conference on Multiphase Technology: Technology from the Arctic to the Tropics, Banff, Canada, 10–11 June, Vol. 31, 193–205.

Sheikh Mohammad Samiur Rahman is currently working to obtain his MS degree from the University of British Columbia (UBC). In addition to his several academic achievements in his undergraduate and graduate degree programs, he has also worked with several companies, including Atkins, Nizine, Teck Resources, and Trinity Mechanical. Rahman's research interests are in the fields of oil and gas, mining, and renewable energy. He holds a BS degree in mechanical engineering from Heriot-Watt University, and he is an active member of the Sustainable Building Science Program at UBC.

Sibi Chacko is a faculty member at Heriot-Watt University. Previously, he specialized in mechanical engineering and worked at various universities, including National Institute of Technology, Calicut, India; King Khalid University, Saudi Arabia; and University Technology Petronas, Malaysia. Chacko's research interests include dynamics, robotics, petroleum, and signal processing.